Annals of Glaciology 38 2004

Experimental and numerical study of granular flow and fence interaction

Thierry FAUG, Mohamed NAAIM, Florence NAAIM-BOUVET
UR ETNA, Cemagref Grenoble, BP 76, 38402 Saint-Martin d'Heres, France
E-mail: thierry.faug@cemagref.fr

ABSTRACT. Dense snow avalanches are regarded as dry granular flows. This paper presents experimental and numerical modelling of deposition processes occurring when a gravity-driven granular flow meets a fence. A specific experimental device was set up, and a numerical model based on shallow-water theory and including a deposition model was used. Both tools were used to quantify how the retained volume upstream of the fence is influenced by the channel inclination and the obstacle height. We identified two regimes depending on the slope angle. In the slope-angle range where a steady flow is possible, the retained volume has two contributions: deposition along the channel due to the roughness of the bed and deposition due to the fence. The retained volume results only from the fence effects for higher slopes. The effects of slope on the retained volume also showed these two regimes. For low slopes, the retained volume decreases strongly with increasing slope. For higher slopes, the retained volume decreases weakly with increasing slope. Comparison between the experiments and computed data showed good agreement concerning the effect of fence height on the retained volume.

1. INTRODUCTION

Besides risk zoning, defence structures such as dams or mounds are used to protect inhabited mountain areas. The interaction between avalanches and obstacles is not fully understood, especially the storing effects. In situ studies continue to be the most direct and certainly the best way to understand and quantify the mechanisms involved in avalanche dynamics and interaction with obstacles. Many instrumented sites including dams exist in various parts of the world. While the results of these studies are awaited, progress continues to be made in related fields, providing a unique source of information for approaching, understanding and modelling avalanche flows. The objective of our research is to determine the hydraulic effects of dams on dry and cohesion-less snow avalanches. Many conceptual behaviour laws have been proposed for snow, but until now none of them has been objectively validated. Recently, interesting scientific progress was made by Pouliquen (1999) for the granular media. This was first achieved for an ideal granular medium (spherical glass beads and unique grain size). This theory was extended to more complex granular media such as polydispersed grains (Chevoir and others, 2001). The dry and cohesion-less snow is usually regarded as granular material; we then considered the Pouliquen effective friction law valid for dry and cohesion-less snow. In this paper, we use a small-scale physical model and numerical model to quantify the effects of dams in terms of retained volumes.

The next section deals with the new deposition mechanism modelling using an empirical friction law. The simple laboratory experiments we performed are described in section 3. Experimental and numerical results are compared in section 4.

2. DEPOSITION MECHANISM: MODELLING

The granular flow is here simulated using a depth-averaged model. The model uses the theory proposed by Savage and Hutter (1989) and the friction law proposed by Pouliquen (1999). An entrainment and deposition model was developed and implemented, and was used to simulate avalanche flows and their interaction with obstacles (Naaim and others, 2003). In the following one-dimensional equations, h is the flow depth and u is the depth-averaged velocity:

$$\frac{\partial h}{\partial t} + \frac{\partial hu}{\partial x} = \phi_{e/d} \tag{1}$$

$$\frac{\partial hu}{\partial t} + \alpha \frac{\partial hu^2}{\partial x} + kgh\cos\theta \frac{\partial h}{\partial x} = gh\sin\theta - \mu(h,u)gh\cos\theta\,\mathrm{sign}(u). \tag{2}$$

α is related to the velocity profile across the layer. Its effect is not significant in this model. We took α equal to 1. k is the ratio of the vertical normal stress to the horizontal normal stress. The isotropy is assumed here and $k = 1$. θ is the slope angle and $\mu(u,h)$ is the effective friction coefficient described in section 2.1. $\phi_{e/d}$ is the erosion–deposition flux detailed in Naaim and others (2003).

The system takes into account the deposition process thanks to the mass-conservation equation. When a given infinitesimal layer (Δh) is deposited, its momentum is transferred to the ground. The new momentum of the moving mass is $(h - \Delta h)u$ which corresponds to decreasing momentum. This is automatically taken into account by our conservative formulation of the shallow-water equations. Neither source nor sink of momentum is needed in this formulation.

https://doi.org/10.3189/172756404781814870 Published online by Cambridge University Press

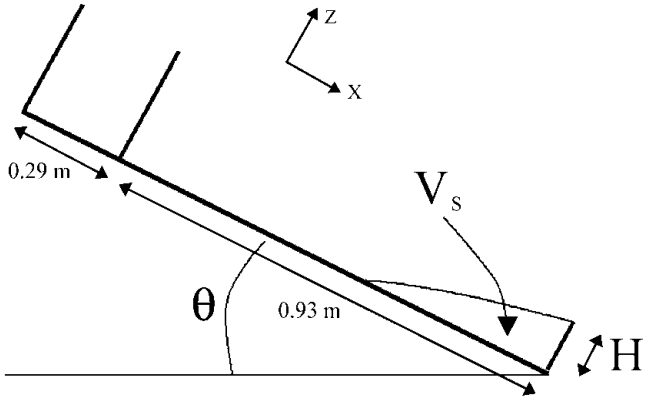

Fig. 1. Schematic view of the experimental-up.

2.1. Friction law

The friction law used is from Pouliquen (1999). The effective friction coefficient is written as:

$$\text{If } \frac{u}{\sqrt{gh}} > 0.136 \text{ then } \mu = \mu_{\min} + (\mu_{\max} - \mu_{\min})\mathrm{e}^{-B\frac{h\sqrt{gh}}{u}}$$

$$\text{If } \frac{u}{\sqrt{gh}} < 0.136 \text{ then } \mu = \mu_{\max},$$

where B, $\mu_{\min} = \tan(\theta_{\min})$ and $\mu_{\max} = \tan(\theta_{\max})$ are parameters depending on the material properties and the bed roughness. B is linked to the parameters β and L defined in Pouliquen (1999) by the following relation: $B = \beta/Ld$, where d is the mean diameter of the particles. We considered that the friction coefficient changes discontinuously at the Froude number $u/\sqrt{gh} = 0.136$, below which steady granular flow has been found to be impossible (Pouliquen, 1999).

2.2. Entrainment and deposition model

The entrainment and deposition model (Naaim and others, 2003) assumes that the erosion/deposition rate is proportional to the excess or deficit shear stress at the bottom and uses the empirical functions $h_{\text{stop}}(\theta)$ (defined in section 4.1) and $h_{\text{start}}(\theta)$. $h_{\text{start}}(\theta)$ is deduced from $h_{\text{stop}}(\theta)$ by $h_{\text{stop}}(\theta) \simeq h_{\text{start}}(\theta + 1^\circ)$.

The deposition model is given by:

$$\phi_{\text{d}} = \frac{2g}{\frac{\partial u}{\partial z}|_{z=0}}\left[\sin(\theta) - \mu(h_{\text{start}}(\theta))\cos(\theta) - k\vec{\nabla}h\cos(\theta)\right]. \quad (3)$$

The erosion model is given by:

$$\phi_{\text{e}} = \frac{2g}{\frac{\partial u}{\partial z}|_{z=0}}\left[\sin(\theta) - \mu(h_{\text{stop}}(\theta))\cos(\theta) - k\vec{\nabla}h\cos(\theta)\right]. \quad (4)$$

In our simulations, we assumed :

$$\frac{\partial u}{\partial z}|_{z=0} = \gamma\frac{u}{h}, \quad (5)$$

corresponding to a linear profile, and we used $\gamma = 1$. Through the extended previous works concerning the vertical velocity profile inside the granular flows (from Savage (1979) to Andreotti and Douady (2001)), different profiles were exhibited. According to the flow and to material conditions, the velocity gradient at the bottom can be higher or smaller than the mean gradient. For simplicity, we approximated the bed velocity gradient by the mean velocity gradient.

The numerical solution of the full equations system is obtained using a finite-volume scheme. The topographic profile is recalculated after each time-step calculation, taking into account the deposition flux. The deposition condition corresponds to the deceleration condition. When it is reached, both deposition and deceleration start to operate. The deceleration decreases the velocity, and the deposition decreases the height. These two processes operate simultaneously and maintain approximately the same shearing rate (u/h) during the stopping process.

2.3. Upstream and downstream boundary conditions

The downstream condition represents the presence of the obstacle. This last is introduced in the model as follows. Three cases are considered:

When h_{t}, the sum of the flow height h and the deposit height h_{d} at the boundary condition, is lower than the obstacle height H, a total reflection of the flow is used.

When the obstacle height is between (h_{t}) and the deposit height (h_{d}), the output flow (Q_{o}) is determined according to the incoming flow (Q_{i}) by:

$$Q_{\text{o}} = Q_{\text{i}}\frac{h + h_{\text{d}} - H}{h}. \quad (6)$$

Finally, when h_{d} exceeds H, the downstream boundary is considered free $(Q_{\text{o}} = Q_{\text{i}})$.

The first and last cases require classical treatment. The intermediate case is not common. The flow is clearly three-dimensional. We roughly simplified the problem by assuming the flow rate proportional to the free area. At the downstream boundary condition, when the flow arrives, the total reflection induces a strong local increase in height. This generates a strong gradient height, which implies the start of deposition according to the deposition model. This process changes the topography till the dam is totally filled with the immobile material. This modification propagates upstream till attaining an equilibrium slope.

3. EXPERIMENTAL SET-UP

The experimental set-up we used consisted of an inclined channel (0.93 m long and 0.2 m wide). A fence of height H was placed at the channel downstream end. A fixed volume of granular material was stored in a box (0.29 m long and 0.2 m wide) situated at the top of the channel. The granular mass was released from the box, and the volume stored upstream of the fence was measured. The granular material comprised glass beads with a mean diameter of 1 mm.

Our study investigated the influence of two parameters on the stored volume V_{s}: (i) the channel inclination θ, and (ii) the fence height H. A schematic view of the experimental set-up can be seen in Figure 1.

4. RESULTS ANALYSIS

4.1. Empirical friction-law parameters

As seen in section 2, empirical friction parameters are needed for implementation in the numerical model. The

https://doi.org/10.3189/172756404781814870 Published online by Cambridge University Press

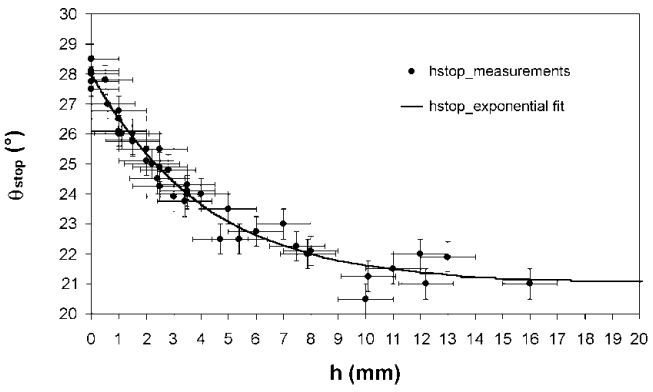

Fig. 2. Variation of the stopping angle as a function of the thickness h. This curve was obtained for glass beads 1 mm in diameter and flowing down a rough plane with sandpaper roughness. Uncertainties were estimated around $\Delta\theta = 0.5°$ *for the slope angle and* $\Delta h = 1$ *mm for the thickness h of the granular layer.*

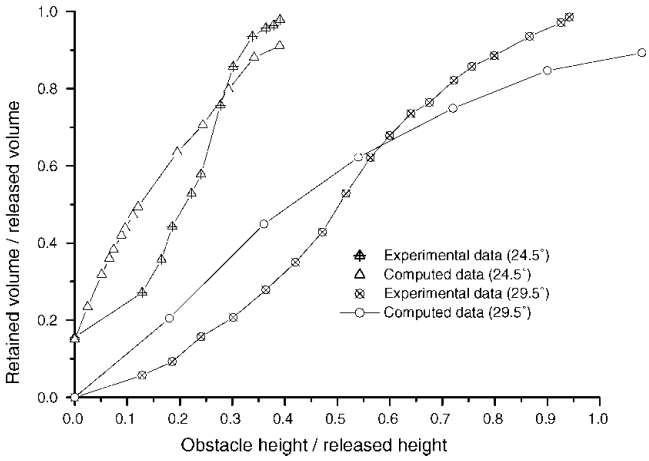

Fig. 3. The retained volume and initial volume ratio according to obstacle height and initial height ratio: comparison between the computed and observed data for two slope angles, 24.5° *and* 29.5°.

function $h_{\mathrm{stop}}(\theta)$ corresponding to the thickness of the granular layer left by a steady uniform flow at the inclination θ was determined empirically by a specific experimental procedure detailed in Pouliquen and Renaut (1996), Daerr and Douady (1999), Pouliquen (1999) and Pouliquen and Forterre (2002).

The granular material used was glass beads flowing down a sandpaper roughness. The $h_{\mathrm{stop}}(\theta)$ empirical function corresponding to our experimental conditions is given in Figure 2. The value of $\theta_{\max}$ corresponding to $h_{\mathrm{stop}} = 0$ was determined accurately and was found to be equal to $\theta_{\max} = 28 \pm 0.5°$. Several couples $(\theta_{\min}, B)$ can be used to fit the experimental data with the equations in section 2.1. The extreme values we obtained lead to:

$\theta_{\min} = 20°$ and $B = 27\mathrm{m}^{-1}$

$\theta_{\min} = 22°$ and $B = 43\mathrm{m}^{-1}$.

The following parameters were used to describe the friction law implemented in the numerical model: $\mu_{\max} = 0.53$ $(\theta_{\max} = 28°)$, $\mu_{\min} = 0.38$ $(\theta_{\min} = 21°)$ and $B = 34\mathrm{m}^{-1}$.

4.2. Influence of the obstacle height

The empirical friction law implies three distinct types of deposition mechanism:

$\theta < \theta_{\min}$: the entire released volume is deposited before interacting with the fence. This case wasn't therefore treated;

$\theta_{\min} < \theta < \theta_{\max}$: a steady regime can be reached before the flow reaches the fence. The volume stored behind the dam comes from two contributions: the volume retained by the dam, and the volume stored along the channel. The latter is represented by the function $h_{\mathrm{stop}}(\theta)$. In our tests, we chose the slope corresponding to the average value: $(\theta_{\max} + \theta_{\min})/2 = 24.5°$;

$\theta > \theta_{\max}$: the volume stored behind the obstacle results only from the obstacle effects $(h_{\mathrm{stop}}(\theta) = 0)$. We chose to study the case of $\theta = 29.5°$.

Experimental and numerical results are presented in Figure 3. The released mass was fixed to 7 kg, and the obstacle height was varied from $H = 1$ cm to $H = 8$ cm. One can observe that the model correctly reproduces the experimental data. However, concavities of numerical and experimental curves are opposite for low obstacle heights, and the error increases when the obstacle height decreases, except for values close to zero where the curves converge: at zero for the case of $\theta > \theta_{\max}$ and at $V_{\mathrm{s}}(h_{\mathrm{stop}}(\theta))/V$ for the other case. The numerical model overestimates the volume stored for low obstacle heights and underestimates it, but less substantially, for higher obstacle heights.

4.3. Influence of the channel inclination

The released mass was 7 kg, and the channel inclination was varied from $\theta = 22°$ to $\theta = 38°$. The ratio of the fence height to the height of the initial volume released, H/h_{i}, was fixed at 0.3 in order not to saturate the volume stored behind the obstacle (V_{s} = released volume) for low slope inclinations. As shown in Figure 4,

the computed data and the experimental data are quite similar and the curves have the same concavities, the slope effect is well reproduced by the model

the computed data overestimate the stored volume

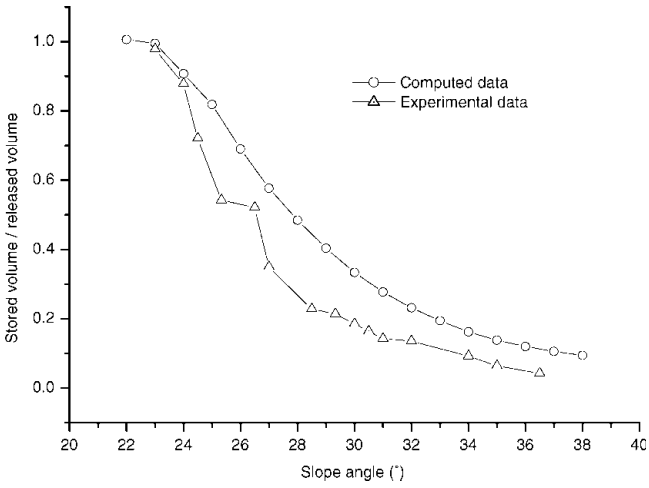

Fig. 4. Retained-volume/initial-volume ratio according to slope angle at fixed initial volume and fixed obstacle height $(H/h_{\mathrm{i}} = 0.3)$.

https://doi.org/10.3189/172756404781814870 Published online by Cambridge University Press

starting from the same value at low slope angle (22°), when the slope angle increases, the computed data decrease more weakly than the observed ones.

However, we have to remember that the friction parameters ($\theta_{\min}, B$) were determined empirically with a significant error for $\theta_{\min}$ ($21° \pm 1°$) and B ($34\,\mathrm{m}^{-1} \pm 7\,\mathrm{m}^{-1}$), as explained in section 4.1. These errors partially explain the discrepancies in Figures 3 and 4. The model was built using quasi-steady uniform conditions, whereas the considered flows are far from these conditions. Furthermore, the impact effect when the front attains the obstacle is not considered in the model. Finally simple boundary-condition treatment was used.

5. CONCLUSION

The presented work, combining numerical and experimental approaches, allowed study of the deposition volume upstream of a fence. Granular material and granular behaviour laws were exploited. For different slope angles and different fence heights, we quantified the retained volume and showed relatively good agreement between the physical experiments and numerical simulations. In the case of dry granular behaviour flowing over a rough bed, we identified two contributions. The first is due to the fence and exists for all the slopes. The second is due to the friction along the rough channel and appears only for slopes where steady flow is possible. This latter modifies significantly the evolution of the retained volume according to the slope angle.

ACKNOWLEDGEMENTS

The authors are grateful to D. Bertrand, P. Lachamp, H. Bellot and F. Ousset who helped in performing the experiments.

REFERENCES

Andreotti, B. and S. Douady. 2001. Selection of velocity profile and flow depth in granular flows. *Phys. Rev. E*, **63**(3), part 2, 31305.

Chevoir, F., M. Prochnow, J. T. Jenkins and P. Mills. 2001. Dense granular flows down an inclined plane. *In* Kishino, Y. *ed.* Powder and grains. Lisse, Swets and Zeitlinger, 373–376.

Daerr, A. and S. Douady. 1999. Two types of avalanche behavior in granular media. *Nature*, **399** (6733), 241–243.

Naaim, M., T. Faug and F. Naaim-Bouvet. 2003. Dry granular flow: erosion and deposition modeling. *Surv. Geophys.*, **24**(516), 569–585.

Pouliquen, O. 1999. Scaling laws in granular flows down rough inclined planes. *Phys. Fluids*, **11**(3), 542–548.

Pouliquen, O. and Y. Forterre. 2002. Friction law for dense granular flows: application to the motion of a mass down a rough inclined plane. *J. Fluid Mech.*, **453**, 133–151.

Pouliquen, O. and N. Renaut. 1996. Onset of granular flows on an inclined rough surface: dilatancy effects. *J. Phys. II France*, **6**, 923–935.

Savage, S. B. 1979. Gravity flows of cohesionless granular materials in chutes and channels. *J. Fluid Mech.*, **92**, 53–96.

Savage, S. B. and K. Hutter. 1989. The motion of a finite mass of granular material down a rough incline. *J. Fluid Mech.*, **199**, 177–215.

https://doi.org/10.3189/172756404781814870 Published online by Cambridge University Press